Clim Dyn (2009) 32:429–440
DOI 10.1007/s00382-008-0387-5

Spatial dependence of diurnal temperature range trends on precipitation from 1950 to 2004

Liming Zhou · Aiguo Dai · Yongjiu Dai · Russell S. Vose · Cheng-Zhi Zou · Yuhong Tian · Haishan Chen

Received: 26 September 2007 / Accepted: 20 February 2008 / Published online: 7 March 2008

Abstract This paper analyzes the spatial dependence of annual diurnal temperature range (DTR) trends from 1950–2004 on the annual climatology of three variables: precipitation, cloud cover, and leaf area index (LAI), by classifying the global land into various climatic regions based on the climatological annual precipitation. The regional average trends for annual minimum temperature (T_{min}) and DTR exhibit significant spatial correlations with the climatological values of these three variables, while such correlation for annual maximum temperature (T_{max}) is very weak. In general, the magnitude of the downward trend of DTR and the warming trend of T_{min} decreases with increasing precipitation amount, cloud cover, and LAI, i.e., with stronger DTR decreasing trends over drier regions. Such spatial dependence of T_{min} and DTR trends on the climatological precipitation possibly reflects large-scale effects of increased global greenhouse gases and aerosols (and associated changes in cloudiness, soil moisture, and water vapor) during the later half of the twentieth century.

Keywords Climate change and variability · DTR · Cloud cover · Precipitation · Land cover

L. Zhou (✉)
School of Earth and Atmospheric Sciences,
Georgia Institute of Technology,
311 Ferst Drive, Atlanta, GA 30332, USA
e-mail: lz35@mail.gatech.edu; lmzhou@eas.gatech.edu

A. Dai
National Center for Atmospheric Research,
P. O. 3000, Boulder, CO 80307, USA

Y. Dai
School of Geography, Beijing Normal University,
100875 Beijing, China

R. S. Vose
Climate Analysis Branch, National Climatic Data Center,
Asheville, NC 28801, USA

C.-Z. Zou
Office of Research and Applications,
NOAA/NESDIS, Camp Springs, MD 20746, USA

Y. Tian
IMSG at NOAA/NESDIS, Camp Springs,
MD 20746, USA

H. Chen
Jiangsu Key Laboratory of Meteorological Disaster,
Nanjing University of Information Science and Technology,
210044 Nanjing, China

1 Introduction

The diurnal temperature range (DTR) has decreased over many land areas since 1950 resulting mostly from a larger increase in minimum air temperature (T_{min}) relative to maximum air temperature (T_{max}) (Easterling et al. 1997; IPCC 2001). This reduction of DTR ($=T_{max} - T_{min}$) has been mainly attributed to increases of cloud cover, precipitation, and soil moisture (Karl et al. 1993; Dai et al. 1997, 1999). Changes in atmospheric circulations and land cover/use, and increases in greenhouse gases and aerosols could also play a role through their impacts on cloudiness and soil moisture or through changes in land surface properties (e.g., Karl et al. 1993; Stenchikov and Robock 1995; Mitchell et al. 1995; Hansen et al. 1995; Collatz et al. 2000; Stone and Weaver 2003; Zhou et al. 2004; Dai et al. 2006; Huang et al. 2006). The DTR trend has, however, weakened during the last 20 years or so (Vose et al. 2005; Dai et al. 2006).

The damping effects on DTR by clouds, soil moisture, greenhouse gases, and aerosols all result from the diurnal

asymmetry in their impact on surface energy balance. The nighttime T_{min} is largely controlled by net longwave radiation while the daytime T_{max} is strongly affected by surface solar heating and the partitioning of sensible and latent heat fluxes (Dai et al. 1999). Clouds, especially thick low clouds, greatly reduce T_{max} and DTR by reflecting sunlight. Soil moisture also damps T_{max} and thus DTR by enhancing evaporative cooling through evapotranspiration. The negative correlation between DTR and precipitation (Dai et al. 1997) results mainly from precipitation's association with cloudiness and soil moisture. On daily to seasonal time scales, clouds are most efficient in reducing DTR but soil moisture also decreases DTR. When averaged over large areas at longer time scales, precipitation should be well correlated with cloudiness and soil moisture and thus can strongly correlate with DTR (Dai et al. 1999).

Observed changes in precipitation have been physically related to those in temperature at both regional and large scales (Madden and Williams 1978; Trenberth and Shea 2005; Nicholls 2004; Trenberth et al. 2007). Trenberth and Shea (2005) indicated that strong negative correlations dominate over land in the warm season, as dry conditions are associated with more sunshine and less evaporative cooling while wet summers often have cool temperatures; positive correlations dominate at high latitudes in winter as warm moist advection in extratropical cyclones favors precipitation and the water holding capacity of the atmosphere limits precipitation amounts in cold conditions. Nicholls (2004) showed that mean T_{max} and T_{min} during the 2002 Australian drought were much higher than during the previous droughts.

Considering the temperature/precipitation relationships, one might expect that the spatial pattern and magnitude of the observed long-term trends in DTR should be strongly related to those in precipitation (and also cloud cover and soil moisture). This paper analyzes the spatial dependence of the observed long-term temperature trends (T_{max}, T_{min}, and DTR) over land for the period 1950–2004 on precipitation, cloud cover, leaf area index (LAI), and land cover type. We found a spatial decoupling between the observed DTR trends and the trends of precipitation/cloudiness over some regions. Instead, there is a strong global connection between the long-term DTR trends and the *climatology* of precipitation, clouds, and LAI by climatic regions. Such connection may provide information about the relative contribution of natural and anthropogenic factors to the observed long-term downward trends in DTR at large spatial scales.

2 Data and methods

A global land surface air temperature (°C) dataset of monthly mean T_{max}, T_{min}, and DTR at 5° longitude × 5° latitude grid boxes was created using monthly records from 7018 meteorological stations over the world for the period 1950–2004 (Vose et al. 2005). It covers 71% of the total land area, 17% more than in previous studies (Easterling et al. 1997). Homogeneity adjustment and data quality assurance were first performed for the time series at each station using techniques of Peterson et al. (1998) and Menne and Williams (2005). The grid-box time series anomalies were derived by averaging station anomaly time series within each box following the method of Jones and Moberg (2003). We temporally averaged the monthly anomalies to generate annual anomalies and then calculated linear trends using least squares fitting.

We used the global monthly land precipitation (mm/day) dataset at 2.5° × 2.5° latitude/longitude grid boxes from Chen et al. (2001), which was created by interpolating gauge observations at over 20,000 stations using the optimal interpolation scheme. Cross validation showed stable and improved performance of the gauge-based analysis for all seasons and over most land areas. We first aggregated the monthly data onto the 5° × 5° grid of the temperature data and then created annual anomalies and the climatology of annual precipitation.

A global monthly total cloud cover (percent sky cover) dataset from 1950 to 2004 at 1° × 1° latitude/longitude grid boxes (Qian et al. 2006) was derived by merging the CRU_TS_2.02 cloud cover data from 1948–2000 (New et al. 2002; Mitchell et al. 2004) and 3-hourly synoptic surface observations from 1975–2004 over 15,000 weather stations and available ship observations (Dai et al. 2006). This merged cloud data was adjusted to have the same mean over a common data period 1977–1993, and are in the form of anomalies with respect to the climatology of the period 1961–1990. Since surface cloud observations over North America are unreliable after 1994 due to widespread use of Automated Surface Observation Systems (ASOS) (Dai et al. 2006), for the period 1995–2004, monthly cloud cover observations from 124 military stations within the contiguous United States were used for those grid boxes overlapping with these stations, while missing values were assigned to the other North American grid boxes with only ASOS observations and no military stations. We first re-mapped the cloud data into the 5° × 5° grid of the temperature data and then created annual anomalies and the climatology of annual cloud cover.

High-quality Moderate Resolution Imaging Spectroradiometer (MODIS) collection four land products of monthly LAI (m^2/m^2) at 0.25° resolution (Myneni et al. 2002) and plant functional types (PFTs) at 1 km resolution (Friedl et al. 2002) were used. The climatology of annual mean LAI was created from 6 years of MODIS LAI products for the period 2001–2006. The MODIS LAIs and PFTs were aggregated onto the 5° × 5° grid of the temperature data. For each grid box, only the primary PFT is considered based on the fractional cover of all PFTs within that box.

After re-mapping all the data onto the 5° × 5° grid box, we selected and used only 528 grid boxes that have at least 7 months data for each year and at least 35 years of data during the period 1950–2004 in all the datasets of temperature, precipitation, LAI, and PFT. As there are very fewer missing data in precipitation, LAI, and PFT, whether or not a grid box was chosen is mainly determined by the availability of its temperature data. For all the chosen boxes, only 3.7% of their annual anomalies from 1950 to 2004 were estimated from 7–11 monthly anomalies instead of using 12 months of data for each year. We assume that uncertainties due to data incompleteness are randomly distributed and thus have minor impacts on our results when averaged over large areas. The cloud data have much less coverage before 1971 and thus only 431 grid boxes that overlap these 528 ones satisfy the aforementioned data length requirement. The use of 7-month and 35-year thresholds is a reasonable compromise between the length of the observing period, data completeness, and spatial coverage.

We considered two cases (A and B) in this study. For Case A, all the 528 grid boxes are used. For Case B, only the 295 grid boxes whose DTR trends in the 55-year period were statistically significant at the 5% level were used. We classified the 528 and 295 grid boxes into 7, 11, 15, 19, and 23 climatic regions, respectively, from dry to wet, in terms of climatological annual precipitation, and then analyzed the spatial dependence of temperature changes on climatological annual precipitation, cloud cover, and LAI by climatic region. For each classification, to ensure comparable samples in each climatic region, we first ranked the annual precipitation of the 528 and 295 grid boxes in ascending order, and then divided them equally into 7, 11, 15, 19, and 23 climatic regions, respectively, each with the about same number of grid boxes. For example, for the classification of 11 (23) climatic regions, each region consists of 48 (∼23) grid boxes for Case A, or of ∼27 (∼13) grid boxes for Case B. In addition, we also examined the spatial dependence of temperature trends on land cover types, which equal 11 climatic regions defined according to the 11 MODIS PFTs.

Spatial averaging of the temperature trends by climatic regions was done using two methods of area-weighted averaging: (1) averaging the trends of all boxes within each region (referred to as Method I) and (2) averaging the annual anomalies of all boxes within each region and then estimating the trend from the averaged time series (referred to as Method II). Similar results are derived from both methods when there are no missing data during the entire period over all grid boxes. However, missing data do exist during part of the period over some boxes and thus both methods are used here. For time series analysis between any two variables, if one variable is missing, another variable is set as missing data too. A two-tailed student's t test was used to test whether linear trends estimated using least squares fitting differ significantly from the zero.

3 Results

3.1 Trends in DTR, precipitation, and cloudiness

Annual T_{max}, T_{min}, and DTR anomalies averaged over the 528 land grid boxes (Case A) from 1950–2004 are shown in Fig. 1. The global mean trends of T_{max}, T_{min}, and DTR are +0.144, +0.216, and −0.072°C per decade, respectively, and are all statistically significant ($p < 0.01$). The strong downward trend of DTR from the 1950s to the 1970s has diminished since about 1983, consistent with previous studies (Vose et al. 2005; Dai et al. 2006). Considering such a DTR change, this study analyzed the temperature trends for three periods, namely 1950–2004, 1950–1983, and 1983–2004.

Figure 2 shows spatial patterns of observed annual DTR trends, together with the corresponding annual cloud cover and precipitation trends and climatological annual cloud cover and precipitation for the 528 grid boxes during the period 1950–2004. Consistent with previous studies (e.g., Vose et al. 2005), the DTR has decreased significantly ($p < 0.05$) over most land areas. The decreasing DTR trend is generally accompanied by increasing cloud cover and/or precipitation over the United States, most of mid-latitude Eurasia, western Australia, and extra-tropical South America, indicating an inverse DTR-clouds/precipitation relationship as reported in previous studies (e.g., Dai et al. 1999). However, most of the largest DTR decrease has occurred over arid and semi-arid regions with the least precipitation and cloud cover such as the West African

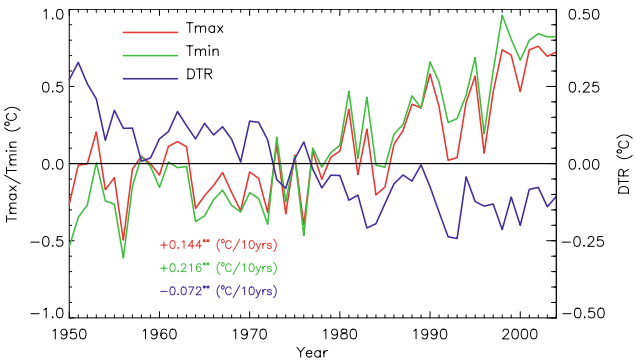

Fig. 1 Annual anomalies of observed T_{max}, T_{min} and DTR averaged over the global 5° by 5° land grid boxes where the data are available for the period 1950–2004. In total, 528 grid boxes with at least 7 months data for each year and at least 35 years of data from 1950 to 2004 were used. The linear trends are listed and those marked with *double asterisks* are statistically significant ($p < 0.01$)

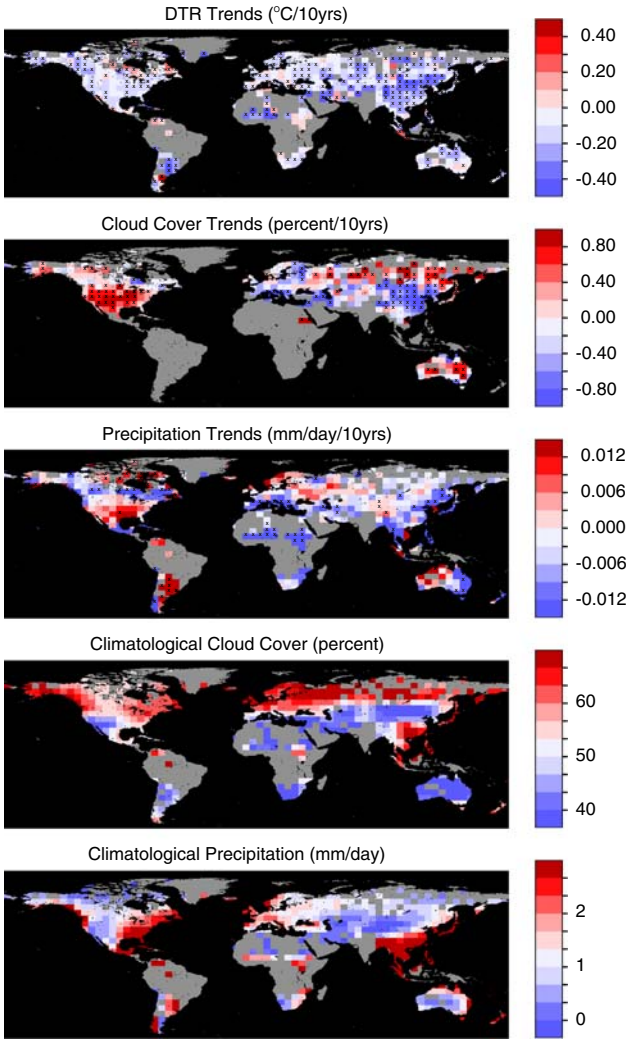

Fig. 2 Spatial patterns of observed annual DTR trends, cloud cover trends, precipitation trends, climatological annual cloud cover, and climatological annual precipitation for the 528 grid boxes defined in Fig. 1. Trends marked with *times symbol* within the grid boxes are statistically significant ($p < 0.05$). Grid boxes in *gray* denote missing values. For the precipitation and cloud cover data, only those grid boxes with the DTR trends and whose precipitation and cloud cover overlap 85% of the DTR for the annual time series during the period 1950–2004 are shown

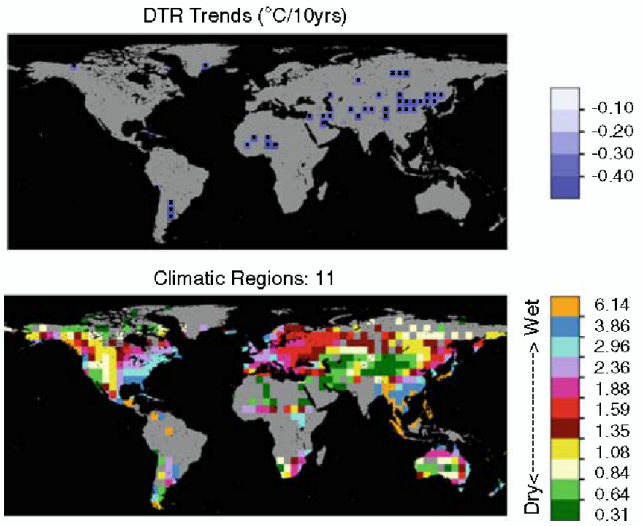

Fig. 3 Spatial pattern of observed annual DTR trend as shown in Fig. 2 but only for those grid boxes whose DTR trends are less than −0.20°C/10 years (*upper panel*). An example of eleven climatic regions defined based on the climatological annual precipitation amount from 1950 to 2004 (*lower panel*)

Sahel, part of the Middle East, and North China, where a coincident decreasing trend in precipitation and/or cloud cover is observed. Such geographical patterns are more evident if we plotted only the DTR trends less than −0.20°C/10 years (Fig. 3), which represent the largest DTR decreasing trends from 49 grid boxes or 9.3% of the 528 grid boxes (Case A) shown in Fig. 2. Note that these 49 trends are all statistically significant ($p < 0.05$) and represent 16.6% of all the 295 significant trends (Case B). The Sahel experienced an unprecedented prolonged drought from the 1950s to the 1980s, but observations show strong and significant coincident downward trends of DTR and rainfall during that period, and a reversal of the DTR trend after rainfall (and clouds, and LAI) recovered over this region since the early 1980s (Zhou et al. 2007). The coincident decreasing trends in DTR and clouds/precipitation over China have been noticed before and increased aerosols from air pollution have been suggested as one potential cause for the DTR reduction (e.g., Kaiser 1998; Dai et al. 1999).

The trends of annual DTR, precipitation, and cloud cover for each of the 528 grid boxes shown in Fig. 2 is sorted and plotted in Fig. 4 from dry to wet according to the magnitude of their climatological annual precipitation amount from 1950 to 2004. The DTR generally declined most over the driest regions. The precipitation decreases over many areas with the largest reduction over the wettest regions. The cloud cover exhibits a substantial spatial variability and does not show an apparent trend from dry to wet regions. Again, the grid by grid pattern of DTR changes is generally inconsistent with that of precipitation and cloud cover as a coupling is expected between the decreasing DTR trends and the increasing precipitation/cloudiness trends (e.g., Dai et al. 1999).

The trends of DTR, cloud cover, and precipitation for the period 1950–1983 (at least 20 years data were required to calculate the trends) exhibit results similar to those for the period 1950–2004 (figures not shown). Interestingly, the largest DTR reduction during this period in the U.S. is also located in the arid and semi-arid regions of the western US. For the period 1983–2004, fewer grid boxes show a significant DTR trend (at least 15 years data were required to calculate the trends), consistent with the diminishing

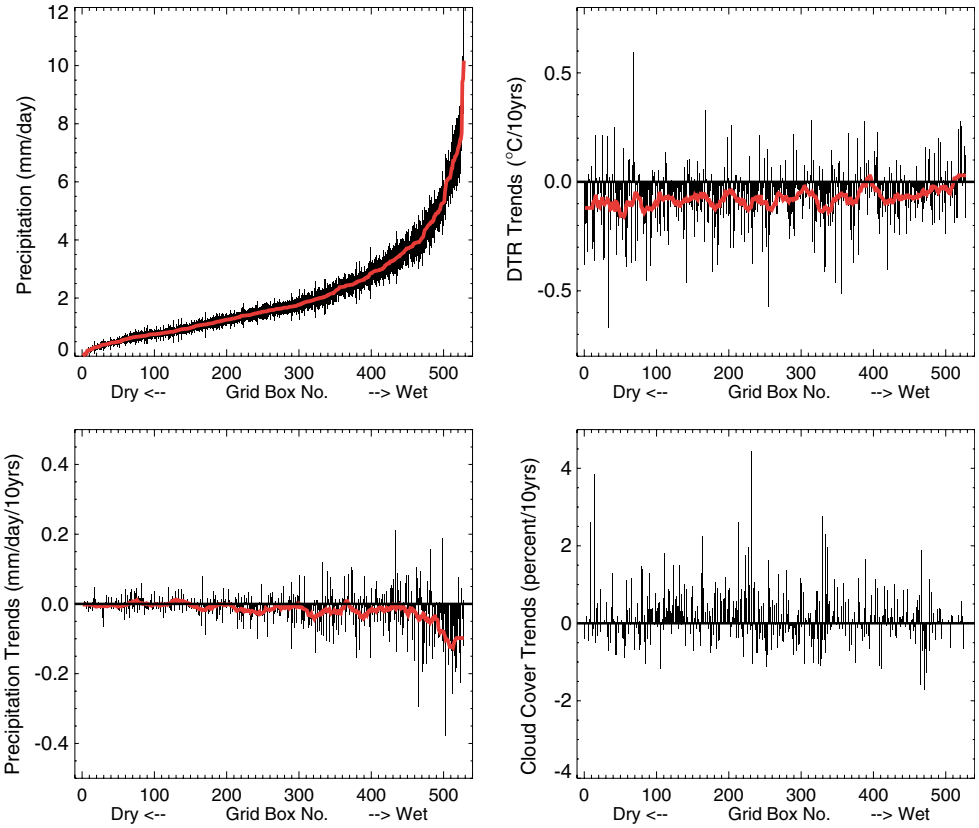

Fig. 4 Climatological annual precipitation in red with one standard deviation range shaded in *black* and trends of annual DTR, precipitation, and cloud cover for the 528 grid boxes shown in Fig. 2, sorted from dry to wet according to the magnitude of their climatological annual precipitation amount from 1950 to 2004. The *solid red lines* overlapping the trends denote the 21-point running area-weighted average (except for the cloud data because of the existence of missing data over some grid boxes)

DTR trend (Vose et al., 2005), and thus no apparent spatial dependence of DTR on precipitation is observed. Whether or not the muted DTR trend since 1983 is a short-term variability of the long-term DTR decreasing trend is unknown. Considering that the 22-year period (1983–2004) may be too short to detect a trend, especially the spatial coverage of the temperature data drops sharply from 70% in 2000 to 48% in 2004 (Vose et al. 2005), our analyses and results applied mainly to the longest period 1950–2004.

3.2 Spatial dependence of temperature trends on climatic regions

Figure 3 shows an example of our classification of eleven climatic regions based on the climatological precipitation between 1950–2004. Figure 5 shows the spatial dependence of regional average trends of annual T_{max}, T_{min}, and DTR on the regional average climatological annual precipitation by climatic region using Method I for Case A. There is a statistically significant correlation ($p < 0.01$) between the precipitation and the trends of T_{min} and DTR, while the correlation between the precipitation and the T_{max} trend is weak. The trend of T_{min} (DTR) generally decreases (increases) linearly with the precipitation, indicating that the lower the precipitation, the stronger the warming in T_{min} and the larger the DTR reduction. In other

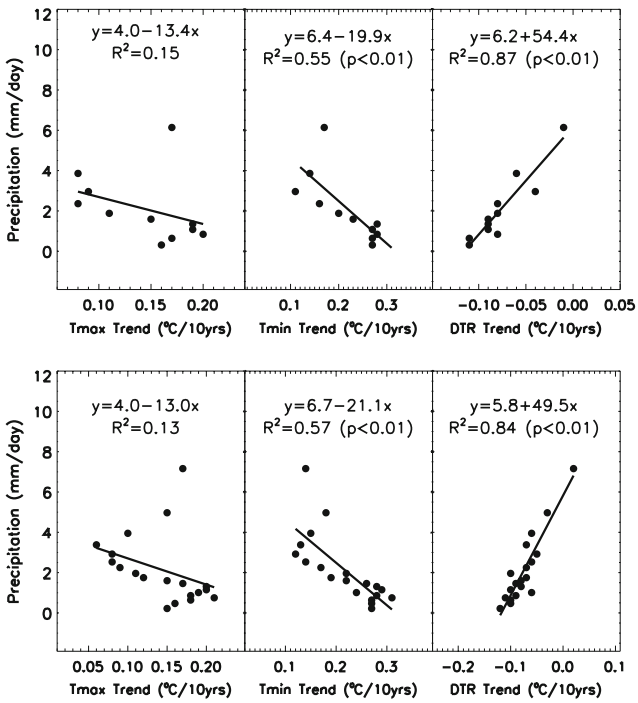

Fig. 5 Dependence of regional average trends of annual T_{max}, T_{min} and DTR on regional average climatological annual precipitation by climatic region for Case A during the period 1950–2004. Here only the results for the 11 (*upper panels*) and 19 (*lower panels*) climatic regions are shown. A linear regression line was fit between the precipitation and the temperature trends. Spatial averaging of Method I was used

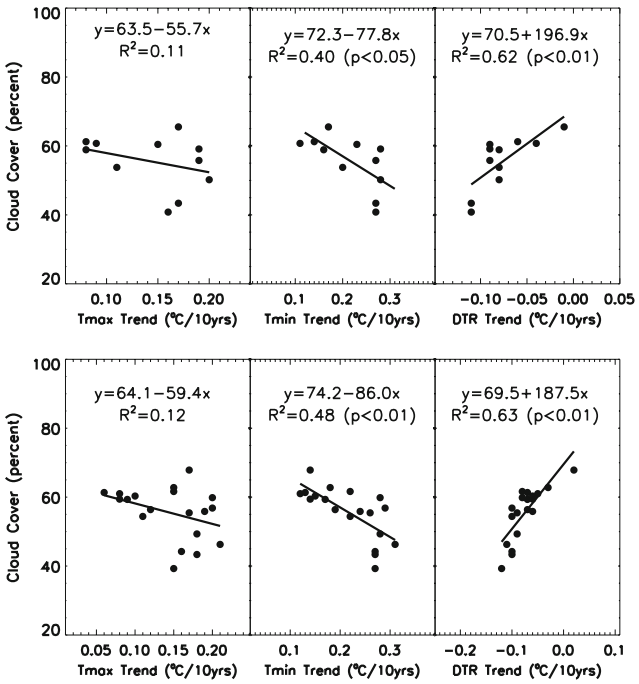

Fig. 6 Same as Fig. 5 but for climatological annual cloud cover

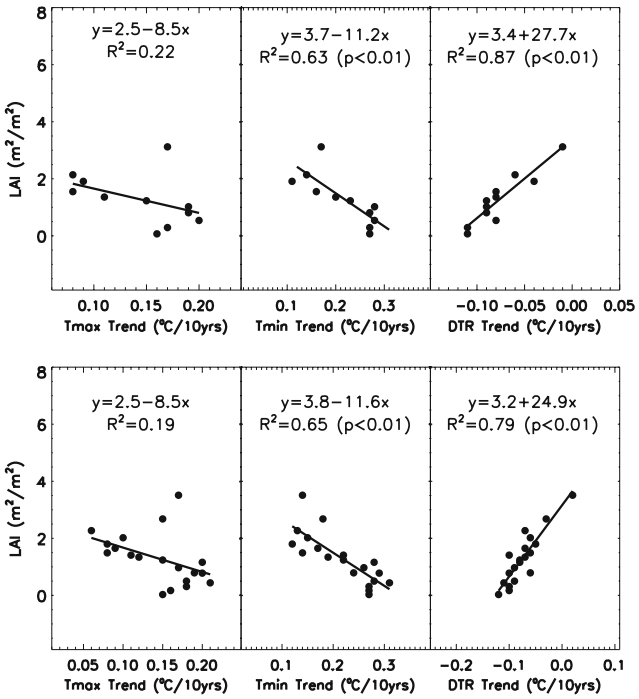

Fig. 7 Same as Fig. 5 but for climatological annual LAI

words, the warming of T_{min} and the reduction of DTR are largest over arid and semi-arid regions. Similar dependence of temperature trends on climatological annual cloud cover and LAI by climatic regions are seen in Figs. 6 and 7. The trend of T_{min} (DTR) generally decreases (increases) linearly with the increase of LAI and clouds, indicating that the warming of T_{min} and the reduction of DTR are strongest over the regions with the least vegetation or cloud cover.

Table 1 Correlation coefficients between regional average annual temperature trends (T_{max}, T_{min}, and DTR) from 1950 to 2004 and regional average climatological annual precipitation, LAI, and cloud cover by climatic region

	Number of Regions	Case A			Case B		
		T_{max}	T_{min}	DTR	T_{max}	T_{min}	DTR
Precipitation							
Method I	7	−0.49	**−0.80**	**0.96**	−0.33	**−0.82**	**0.94**
	11	−0.39	**−0.75**	**0.93**	−0.20	**−0.74**	**0.97**
	15	−0.41	**−0.73**	**0.80**	−0.32	**−0.73**	**0.80**
	19	−0.36	**−0.75**	**0.92**	−0.35	**−0.70**	**0.77**
	23	−0.37	**−0.72**	**0.81**	−0.17	**−0.71**	**0.75**
Method II	7	−0.56	**−0.79**	**0.94**	−0.42	**−0.81**	**0.92**
	11	−0.45	**−0.74**	**0.89**	−0.30	**−0.74**	**0.94**
	15	−0.47	**−0.72**	**0.71**	−0.37	**−0.72**	**0.80**
	19	−0.42	**−0.72**	**0.83**	−0.42	**−0.70**	**0.76**
	23	**−0.43**	**−0.71**	**0.75**	−0.26	**−0.71**	**0.77**
LAI							
Method I	7	−0.57	**−0.85**	**0.95**	−0.40	**−0.86**	**0.93**
	11	−0.47	**−0.80**	**0.94**	−0.26	**−0.79**	**0.96**
	15	−0.49	**−0.78**	**0.79**	−0.39	**−0.78**	**0.78**
	19	−0.45	**−0.80**	**0.89**	−0.39	**−0.73**	**0.77**
	23	**−0.44**	**−0.76**	**0.80**	−0.22	**−0.74**	**0.73**
Method II	7	−0.59	**−0.85**	**0.93**	−0.48	**−0.81**	**0.93**
	11	−0.50	**−0.80**	**0.94**	−0.35	**−0.79**	**0.95**
	15	−0.47	**−0.79**	**0.84**	−0.29	**−0.76**	**0.88**
	19	**−0.50**	**−0.78**	**0.81**	−0.21	**−0.76**	**0.86**
	23	**−0.47**	**−0.76**	**0.72**	−0.26	**−0.74**	**0.80**
Cloud cover							
Method I	7	−0.41	−0.66	**0.81**	−0.32	−0.72	**0.77**
	11	−0.34	**−0.64**	**0.79**	−0.22	**−0.68**	**0.79**
	15	−0.41	**−0.68**	**0.71**	−0.26	**−0.61**	**0.65**
	19	−0.38	**−0.69**	**0.79**	−0.28	**−0.58**	**0.61**
	23	−0.30	**−0.60**	**0.72**	−0.16	**−0.57**	**0.55**
Method II	7	−0.40	−0.67	**0.88**	−0.38	−0.66	**0.79**
	11	−0.33	**−0.63**	**0.85**	−0.28	**−0.68**	**0.85**
	15	−0.32	**−0.60**	**0.73**	−0.19	**−0.63**	**0.79**
	19	−0.40	**−0.66**	**0.74**	−0.15	**−0.60**	**0.69**
	23	−0.28	**−0.59**	**0.69**	−0.21	**−0.60**	**0.66**

Correlation coefficients were estimated as in Fig. 5. Coefficients in *bold* are statistically significant ($p < 0.05$)

Table 1 lists the correlation coefficients between the regional average annual temperature trends and the regional average climatological annual means of cloud cover, precipitation, and LAI by climatic regions using both Method I and II for both Case A and B during the period 1950–2004. Almost all of the coefficients for T_{min} and DTR

Table 2 Average trends (°C/10 years) of annual T_{max}, T_{min}, and DTR from 1950 to 2004 by PFT

	PFT Type[a]	Case A				Case B			
		Grids[b]	T_{max}	T_{min}	DTR	Grids[b]	T_{max}	T_{min}	DTR
Method I	1	82	0.17	0.20	−0.03	40	0.17	0.22	−0.05
	2	53	0.14	0.16	−0.03	38	0.15	0.18	−0.05
	3	21	0.29	0.39	−0.11	15	0.27	0.41	−0.16
	4	40	0.11	0.17	−0.06	23	0.10	0.19	−0.09
	5	137	0.14	0.21	−0.06	69	0.12	0.24	−0.12
	6	62	0.13	0.22	−0.09	31	0.13	0.28	−0.16
	7	71	0.12	0.23	−0.10	41	0.09	0.25	−0.16
	8	16	0.12	0.21	−0.09	10	0.10	0.26	−0.16
	9	41	0.13	0.27	−0.15	25	0.11	0.33	−0.22
Method II	1	82	**0.17**	**0.20**	**−0.03**	40	**0.17**	**0.22**	**−0.05**
	2	53	**0.13**	**0.17**	**−0.04**	38	**0.14**	**0.19**	**−0.06**
	3	21	**0.29**	**0.38**	**−0.09**	15	**0.24**	**0.42**	**−0.20**
	4	40	**0.12**	**0.18**	**−0.06**	23	**0.10**	**0.19**	**−0.09**
	5	137	**0.15**	**0.21**	**−0.06**	69	**0.14**	**0.26**	**−0.12**
	6	62	**0.13**	**0.22**	**−0.09**	31	**0.13**	**0.29**	**−0.16**
	7	71	**0.14**	**0.24**	**−0.10**	41	**0.10**	**0.26**	**−0.16**
	8	16	**0.11**	**0.22**	**−0.11**	10	**0.10**	**0.26**	**−0.16**
	9	41	**0.14**	**0.27**	**−0.13**	25	**0.12**	**0.32**	**−0.21**

Trends in *bold* are statistically significant ($p < 0.05$)

[a] PFT Evergreen needleleaf trees (1), evergreen broadleaf trees (2), deciduous needleleaf trees (3), deciduous broadleaf trees (4), shrub (5), grass (6), cereal crop (7), broadleaf crop (8), barren or sparse vegetation (9)

[b] PFT with less than ten grid boxes are not listed

are statistically significant ($p < 0.05$), and the correlation between the temperature trends and the cloud cover is slightly weaker than that between the temperature trends and the precipitation and LAI. Similar results are seen for the period 1950–1983 but not for the period 1983–2004 (not shown for simplicity). Such change during these two periods is expected as most of the grid boxes show a decreasing DTR trend before 1983 but fewer significant DTR trends after 1983 as discussed previously.

Table 2 lists regional average trends of annual T_{max}, T_{min}, and DTR by PFT using both Method I and II for both Case A and B during the period 1950–2004. The decreasing DTR trend is generally large for short vegetation (e.g., shrubs, grasses, crops) and small for dense forests (e.g., evergreen needleleaf trees, evergreen broadleaf trees, deciduous broadleaf trees). It is largest for barren and sparse vegetation (PFT 9), smallest for evergreen needleleaf trees (PFT 1), and in between for other PFTs with intermediate amount of LAI such as grasses, crops, and shrubs, except for deciduous needleleaf trees (PFT 3) which shows a strong reduction in DTR. Such dependence of the DTR trends on PFTs is consistent with the dependence of DTR trends on precipitation and LAI shown previously. It is expected because climate (e.g., precipitation) largely determines the geographical distribution and amount of vegetation.

To test whether our estimated linear trends of temperatures are sensitive to points at the start or end of the annual anomalies, we changed the start date in one-year increment from 1950 to 1960 or the end date from 1994 to 2004, the spatial dependence of T_{max}, T_{min}, and DTR on precipitation shown previously remains robust. We also change the data length required to estimate the linear trends, between 20–40 years, and the results still hold true in most cases.

The above results indicate that most of the observed long-term DTR trends in the last several decades are generally largest over arid and semi-arid areas. They reflect mainly the DTR changes in the Tropics and northern middle latitudes as few grid boxes in the Southern Hemisphere have DTR data and the contribution from northern high-latitudes are relatively small due to their small areas.

3.3 Relations between DTR and precipitation/cloudiness time series

We analyzed interannual variations and linear trends of annual T_{max}, T_{min}, and DTR anomalies and their association with precipitation and clouds at the global scale and by climatic regions. Figure 8 shows the global average annual anomalies of DTR, precipitation, and cloud cover from 1950–2004. All variables show a significant trend ($p < 0.01$), −0.072°C/10 years for DTR, −0.021 mm/day per 10 years for precipitation, and 0.118%/10 years for cloud cover, respectively. Note that the cloud data were averaged from fewer grid boxes than the DTR and precipitation data, especially before 1971. Relative to the long-term decreasing trends, one can see an inverse correlation between DTR and precipitation/clouds. Simply

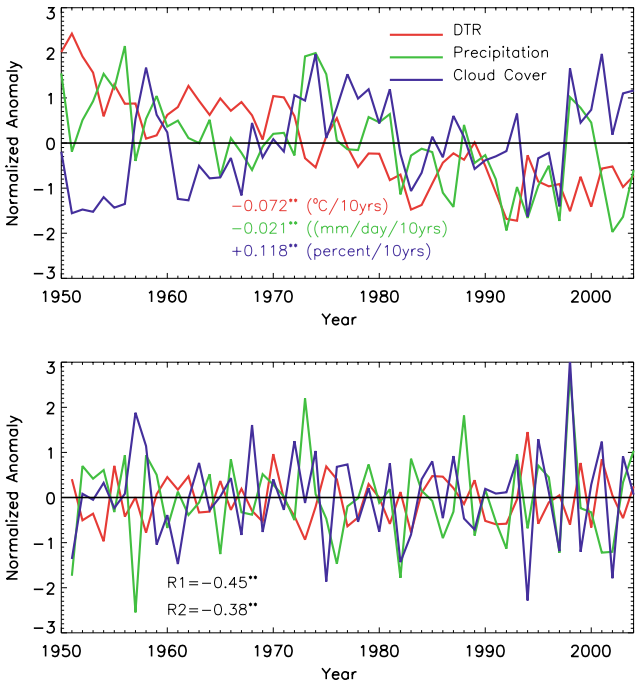

Fig. 8 Global average annual anomalies of DTR, precipitation, and cloud cover from 1950 to 2004 (*upper panel*) and their differentiated time series (i.e., detrending the original time series) (*lower panel*) for the 528 grid boxes defined in Fig. 1. Note that the cloud data were averaged from fewer grid boxes than the DTR and precipitation data, especially before 1971. The linear trends and correlation coefficients (R) are listed and those marked with *asterisk* (*double asterisks*) are statistically significant at $p < 0.05$ ($p < 0.01$). R was calculated after differentiating the original time series (R1 is the correlation between the DTR and the precipitation and R2 is the correlation between the DTR and the cloud cover). The time series of data were normalized by subtracting their mean divided by their standard deviation (for visualization purpose only)

correlating the temperature and clouds/precipitation time series as shown in Fig. 8 to quantify their relationship may result in spurious association due to the presence of strong trends (sustained upward or downward movements) in the time series (Granger and Newbold, 1974; Gujarati 1995). To reduce the possibility of such spurious association, we differentiated the original time series (i.e., removing the linear trends) and then estimated the relationship between changes in temperatures and changes in precipitation/cloudiness (Fig. 8). For example, after differentiating the original time series, the new DTR time series represent DTR changes relative to the previous year. Evidently, there is a statistically significant negative correlation between the changes in DTR and the change in clouds/precipitation, consistent with previous studies (e.g., Karl et al. 1993; Dai et al. 1999).

Figure 9 shows the time series of regional average annual DTR and precipitation from 1950–2004 for three climatic regions representing the driest, intermediate, and wettest in terms of seven climatic regions classified. Figure 10 shows the same except for changes in DTR versus cloud cover. The DTR shows statistically significant negative linear trends ($p < 0.01$) for all regions, with a magnitude decreasing from dry to wet. Precipitation exhibits significant trends in most regions while cloud cover has insignificant trends in most regions. In general, relative to the long-term decreasing trend in DTR and/or trends in precipitation and clouds if any, one can see an inverse correlation between DTR and precipitation/clouds over all regions. After the original time series were differentiated as done at the global scale (Fig. 8), there is a statistically significant negative relationship between the changes in DTR and the change in clouds/precipitation ($p < 0.01$) for almost all the climatic regions. Interestingly, the coefficient (β_1) for DTR is largest over the driest region and smallest over the wettest regions, indicating that the effect of given changes in clouds/precipitation on changes in DTR is strongest over arid and semiarid ecosystems.

4 Discussion

Increased cloud cover, precipitation, and soil moisture have been widely used as major factors to explain the worldwide reduction of DTR in the last several decades. If the negative correlation between changes in DTR and changes in clouds/precipitation shown above and in previous studies (e.g., Dai et al. 1999) holds for secular changes, one would expect to see a spatial coupling between the observed long-term decreasing DTR trends and increasing precipitation/clouds trends. The coincident decreasing trends in DTR, clouds and/or precipitation over some regions, such as West Africa (Zhou et al. 2007) and China (Kaiser 1998), where the DTR decreased most (Figs. 2–3), suggest other mechanisms may be involved in changing the DTR at regional scales, such as changes in land surface properties (Zhou et al. 2003, 2004, 2007) and anthropogenic aerosols-induced increases in downward longwave surface forcing (Huang et al. 2006).

DTR can be changed through a number of mechanisms all connected to changes in surface energy and hydrological balances controlled by greenhouse gases, atmospheric composition, water vapor, cloud properties, atmospheric circulations, and surface properties (e.g., soil moisture, vegetation, surface roughness, land use/cover). The diurnal cycle of temperature over land is maintained by daytime solar heating and nighttime radiative cooling. Daytime temperatures are affected less than nighttime temperatures by a given forcing because daytime turbulent mixing is strong and thick and a large portion of the forcing is converted into latent heat through evapotranspiration.

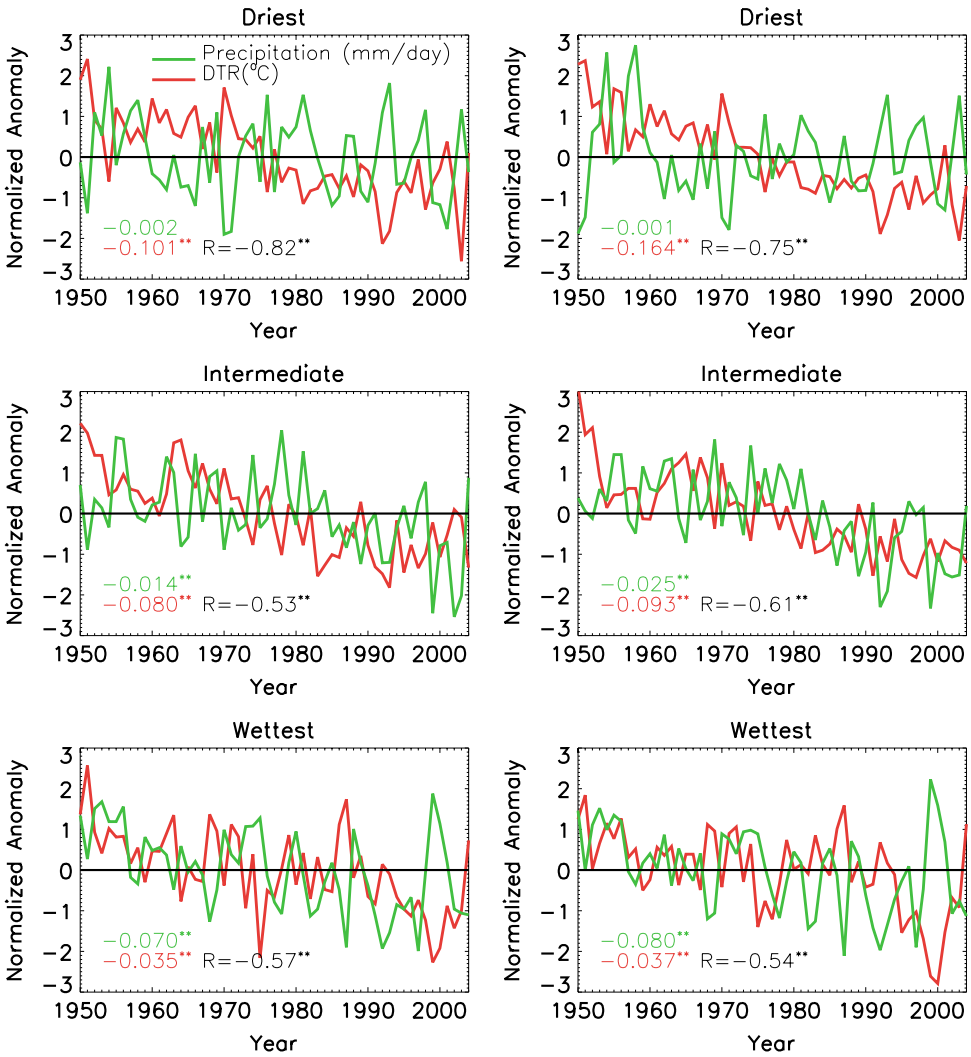

Fig. 9 Normalized regional average anomalies of annual DTR and precipitation from 1950 to 2004 in terms of seven climatic regions. Three of the seven regions, representing the driest (upper panel), intermediate (middle panel), and wettest (*lower panel*) are shown for Case A (*left panels*) and B (*right panels*). The linear trends, correlation coefficients (R), and normalization are defined as in Fig. 8

Consequently, nighttime temperatures (hence DTR) are more sensitive to changes in radiative drivers under cold stable conditions than under warm unstable conditions (IPCC 2007). The statistical analyses in Table 3 indicate that the strongest effect of clouds/precipitation on DTR is over the driest regions, where evaporative cooling during daytime is limited. Dai et al. (1999) observed the largest effects of clouds/precipitation on DTR in warm and dry seasons.

We speculate that the global correlation between the decreasing DTR trends and the climatological precipitation, cloud cover, and LAI shown in Figs. 5–7 might reflect the large-scale effects of increased greenhouse gases and aerosols (and associated changes in cloudiness, precipitation, and water vapor) on DTR over different ecosystems. Its further attribution, however, is beyond the scope of this study. Winter or nighttime temperatures (hence DTR) are strongly correlated with downward longwave radiation (IPCC 2007). In humid and warm regions where the greenhouse effect is very large, adding a small additional amount of greenhouse gases has only a small direct impact on downward infrared radiation, while for the same amount of increase in greenhouse gases, a greater effect is expected over dry and cold regions (IPCC 2007). At regional scales, increased clouds and soil moisture are most effective in controlling short-term DTR changes (e.g., daily to seasonal) while increased greenhouse gases and aerosols are a relatively small forcing compared with that induced by cloudiness changes during the same period over many regions such as the US. (Dai et al. 1999). However, changes in cloud cover and precipitation often have considerable spatial and temporal variability and thus may have no strong long-term trends when averaged at large spatial scales, while the effects of greenhouse gases and aerosols as a steady and global forcing are likely to become more important and thus largely determine the spatial pattern of long-term DTR trends (e.g., multi-decadal to century).

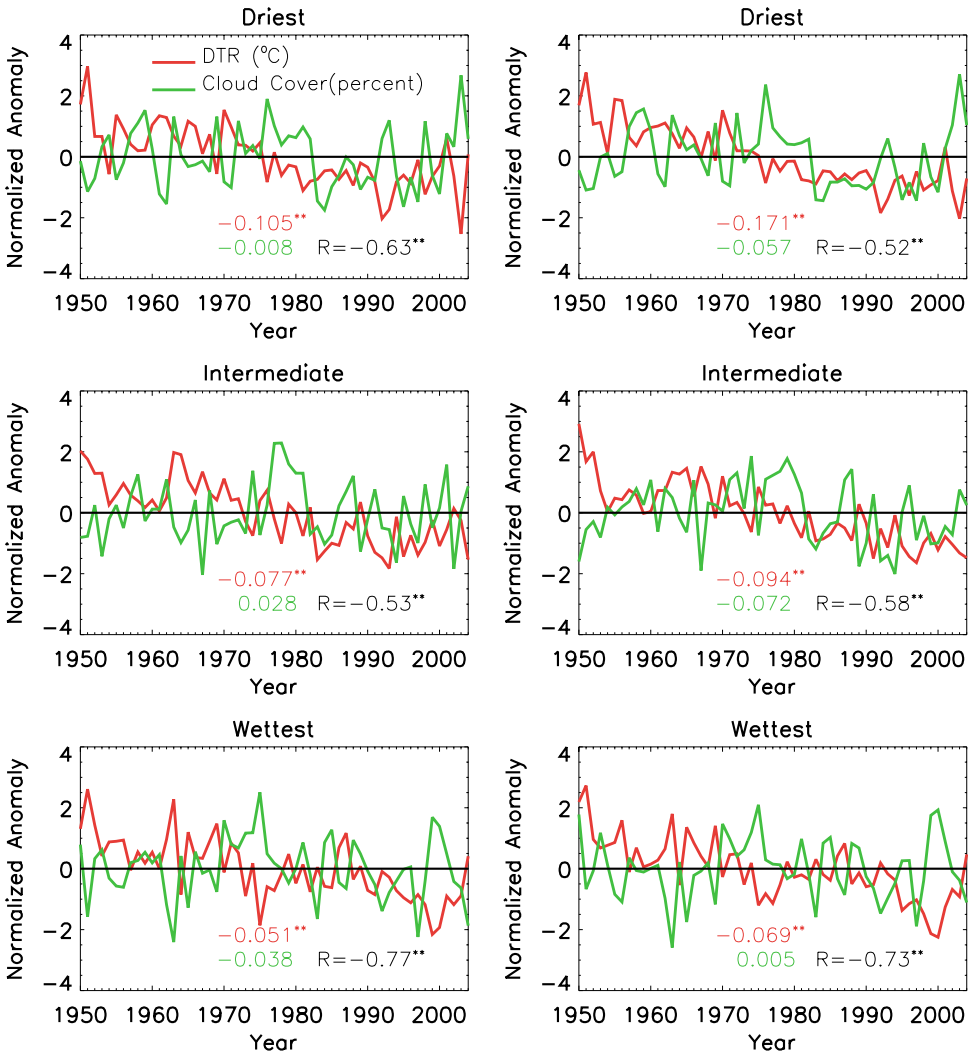

Fig. 10 Same as Fig. 9 but for cloud cover

5 Conclusions

We have analyzed the spatial dependence of long-term trends in T_{max}, T_{min}, and DTR over land for the period 1950–2004 on the climatological annual mean values of precipitation, cloud cover, and LAI among climatic regions defined based on their climatological annual precipitation and by land cover types. The regional average trends for annual minimum (T_{min}) and DTR exhibit significant spatial correlations with the climatological precipitation, cloud cover, and LAI, while such correlation for annual maximum (T_{max}) is very weak. The warming trend of T_{min} and the magnitude of the decreasing DTR trend generally decrease with increasing precipitation amount, cloud cover, and LAI among climatic regions, so that the strongest warming in T_{min} and the largest decreasing DTR trends from 1950 to 2004 are generally observed over dry regions with the least mean precipitation, cloud coverage, and vegetation. In other words, most of the largest decreasing DTR trend from 1950 to 2004 is observed generally over arid and semi-arid regions such as the Sahel and North China where drought has occurred. The global correlation between the decreasing DTR trends and the climatological precipitation/clouds by climatic region may reflect the large-scale effects of increased global greenhouse gases and aerosols (and associated changes in clouds, soil moisture, and water vapor) on DTR.

Although there is a spatial decoupling between the long-term trends in DTR and those in clouds and precipitation over some regions, our statistical analyses indicate that the inverse relationship between DTR and clouds/precipitation reported previously (e.g., Karl et al. 1993; Dai et al. 1999) is robust over almost all regions after the dominant long-term trends are removed, and the effects of given changes in clouds/precipitation on DTR are strongest over arid and semi-arid regions. The observed coincident decreasing trends in DTR and precipitation and/or clouds over some regions where the DTR decreased most suggest that other mechanisms may have been involved in changing the DTR since 1950.

Table 3 Statistical results between changes in DTR (ΔY) and changes in precipitation/clouds (ΔX) for the period 1950–2004

Number of regions	Region #	$\Delta Y = \beta_0 + \beta_1 \Delta X + \varepsilon$							
		Precipitation				Cloud Cover			
		Case A		Case B		Case A		Case B	
		R^2	β_1	R^2	β_1	R^2	β_1	R^2	β_1
7	Driest	0.67	**−0.42**	0.57	**−0.45**	0.40	**−0.11**	0.27	**−0.10**
	Intermediate	0.29	**−0.10**	0.38	**−0.10**	0.28	**−0.07**	0.34	**−0.08**
	Wettest	0.32	**−0.03**	0.30	**−0.02**	0.59	**−0.08**	0.54	**−0.07**
11	Driest	0.54	**−0.45**	0.47	**−0.54**	0.42	**−0.12**	0.49	**−0.13**
	Intermediate	0.29	**−0.10**	0.32	**−0.09**	0.22	**−0.07**	0.22	**−0.07**
	Wettest	0.43	**−0.02**	0.31	**−0.01**	0.61	**−0.07**	0.47	**−0.05**
15	Driest	0.47	**−0.52**	0.40	**−0.59**	0.54	**−0.13**	0.49	**−0.14**
	Intermediate	0.21	**−0.09**	0.34	**−0.10**	0.48	**−0.09**	0.45	**−0.10**
	Wettest	0.29	**−0.01**	0.29	**−0.01**	0.36	**−0.06**	0.32	**−0.04**
19	Driest	0.45	**−0.55**	0.51	**−0.74**	0.61	**−0.15**	0.56	**−0.15**
	Intermediate	0.09	*−0.06*	0.30	**−0.08**	0.43	**−0.08**	0.58	**−0.11**
	Wettest	0.29	**−0.01**	0.09	*−0.01*	0.36	**−0.06**	0.06	−0.02
23	Driest	0.51	**−0.65**	0.37	**−0.69**	0.60	**−0.15**	0.49	**−0.15**
	Intermediate	0.09	*−0.05*	0.38	**−0.09**	0.47	**−0.09**	0.52	**−0.09**
	Wettest	0.25	**−0.01**	0.21	**−0.01**	0.31	**−0.05**	0.16	**−0.03**

The global available 528 (Case A) and 295 (Case B) grid boxes were classified into 7, 11, 15, 19, and 23 climatic regions, respectively, from dry to wet, based on their climatological annual precipitation. For each classification, only three regions, representing the driest, intermediate, and wettest, are shown. Regression coefficients, β_1, in *bold* (*italic*) are statistically significant at the 1% (5%) level

Some uncertainties exist in our calculation of linear and regional average trends and time series analysis because of gaps in spatial coverage and temporal limitations in the data. Our results and conclusions should be representative mainly over the Tropics and northern mid-latitudes where this analysis had the most observations. Given the complex nature of this issue, further investigation and attribution of such spatial dependence of DTR on precipitation and of possible mechanisms for explaining the observed long-term temperature trends (especially $T_{\min}$ and DTR) are needed.

Acknowledgments The authors wish to thank two anonymous reviewers for suggestions that improved the manuscript. This study was supported by the NSF grant ATM-0720619 and the DOE grant DE-FG02-01ER63198. H. Chen was supported by the National Natural Science Foundation of China under grant 40405018 and the Foundation of Jiangsu Key Laboratory of Meteorological Disaster (KLME050205), NUIST, China. Y. Dai was supported by the National Natural Science Foundation of China under grant 40225013 and the 111 Project of Ministry of Education and State Administration for Foreign Experts Affairs of China. The National Center for Atmospheric Research is supported by the National Science Foundation.

References

Chen M, Xie P, Janowiak JE, Arkin PA (2001) Global land precipitation: a 50-year monthly analysis based on gauge observations. J Hydrom 3:249–266

Collatz GJ, Bounoua L, Los SO, Randall DA, Fung IY, Sellers PJ (2000) A mechanism for the influence of vegetation on the response of the diurnal temperature range to changing climate. Geophy Res Lett 27:3381–3384

Dai A, Del Genio AD, Fung IY (1997) Clouds, precipitation, and temperature range. Nature 386:665–666

Dai A, Trenberth KE, Karl TR (1999) Effects of clouds, soil moisture, precipitation, and water vapor on diurnal temperature range. J Clim 12:2451:2473

Dai A, Karl TR, Sun B, Trenberth KE (2006) Recent trends in cloudiness over the United States: a tale of monitoring inadequacies. Bull Am Met Soc 87(5):597–606

Easterling DR et al (1997) Maximum and minimum temperature trends for the globe. Science 277:364–367

Friedl MA et al (2002) Global land cover from MODIS: algorithms and early results. Remote Sens Environ 83:287–302

Granger CWJ, Newbold P (1974) Spurious regressions in econometrics. J Econom 2:111–120

Gujarati DN (1995) Basic econometrics, 3rd edn. McGraw-Hill, New York. ISBN 0-07-025214-9

Hansen J, Sato M, Ruedy R (1995) Long-term changes of the diurnal temperature cycle: implications about mechanisms of global climate change. Atmos Res 37:175–209

Huang Y, Dickinson RE, Chameides WL (2006) Impact of aerosol indirect effect on surface temperature over East Asia. Proc Natl Acad Sci USA 103:4371–4376

IPCC (2001) Climate change 2001: the scientific basis. Cambridge University Press, Cambridge

IPCC (2007) Climate change 2007: the physical science basis, contribution of working group I to the fourth assessment report of the IPCC (ISBN 978 0521 88009-1), Cambridge University Press, Cambridge

Jones PD, Moberg A (2003) Hemispheric and land-scale surface air temperature variations: an extensive revision and an update to 2001. J Clim 16:206–223

Kaiser DP (1998) Analysis of total cloud amount over China. Geophys Res Lett 25(19):3599–3602

Karl T et al (1993) A new perspective on recent global warming: asymmetric trends of daily maximum and minimum temperature. Bull Am Meteorol Soc 74(6):1007–1023

Madden RA, Williams J (1978) The correlation between temperature and precipitation in the United States and Europe. Mon Weather Rev 106:142–147

Menne MJ, Williams CW Jr (2005) Detection of undocumented change point: on the use of multiple test statistics and composite reference series. J Clim 18(20):4271–4286

Mitchell JFB, Davis RA, Ingram WJ, Senior CA (1995) On surface temperature, greenhouse gases, and aerosols: models and observations. J Clim 8:2364–2386

Mitchell KE et al (2004) The multi-institution North American Land Data Assimilation System (NLDAS): utilizing multiple GCIP products and partners in a continental distributed hydrological modeling system. J Geophys Res 109:D07S90. doi: 10.1029/2003JD003823

Myneni RB et al (2002) Global products of vegetation leaf area and fraction absorbed PAR from year one of MODIS data. Remote Sens Environ 83:214–231

New M, Lister D, Hulme M, Makin I (2002) A high-resolution data set of surface climate for terrestrial land areas. Clim Res 21:1–25

Nicholls N (2004) The changing nature of Australian droughts. Clim Change 63:323–336

Peterson TC, Vose RS, Razuvaey VN, Schmoyer RL (1998) Global Historical Climatology Network (GHCN) quality control of monthly temperature data. Int J Climatol 18:1169–1179

Qian T, Dai A, Trenberth KE, Oleson KW (2006) Simulation of global land surface conditions from 1948–2004. Part I: forcing data and evaluation. J Hydrom 7:953–975

Stenchikov GL, Robock A (1995) Diurnal asymmetry of climatic response to increased CO2 and aerosols: forcings and feedbacks. J Geophys Res 100:26211–26227

Stone DA, Weaver AJ (2003) Factors contributing to diurnal temperature range trends in twentieth and twenty-first century simulations of the CCCma coupled model. Clim Dyn 20:435–445

Trenberth KE, Shea DJ (2005) Relationships between precipitation and surface temperature. Geophys Res Lett 32:L14703. doi: 10.1029/2005GL022760

Trenberth KE et al (2007) Observations: surface and atmospheric climate change. In: Solomon S, Qin D, Manning M, Chen Z, Marquis M, Averyt KB, Tignor M, Miller HL (eds) Climate change 2007: the physical science basis. Contribution of working group I to the fourth assessment report of the intergovernmental panel on climate change. Cambridge University Press, Cambridge

Vose RS, Easterling DR, Gleason B (2005) Maximum and minimum temperature trends for the globe: an update through 2004. Geophys Res Lett 32:L23822. doi:10.1029/2005GL024379

Zhou L et al (2003) A sensitivity study of climate and energy balance simulations with use of satellite derived emissivity data over the northern Africa and the Arabian peninsula. J Geophys Res 108(D24):4795. doi:10.1029/2003JD004083

Zhou L et al (2004) Evidence for a significant urbanization effect on climate in China. Proc Natl Acad Sci USA 101(26):9540–9544

Zhou L, Dickinson RE, Tian Y, Vose R, Dai Y (2007) Impact of vegetation removal and soil aridation on diurnal temperature range in a semiarid region—application to the Sahel. Proc Natl Acad Sci USA 104(46):17937–17942